Pulsed LED line light for large-scale PIV—development and use in wave load measurements

OPEN ACCESS
IOP Publishing
Measurement Science and Technology
Meas. Sci. Technol. **32** (2021) 115205 (12pp)
https://doi.org/10.1088/1361-6501/ac17ce

Pulsed LED line light for large-scale PIV—development and use in wave load measurements

W Bakker[1,2,*], B Hofland[1], E de Almeida[1], G Oldenziel[2,3] and E F J Overmars[3]

[1] Department of Hydraulic Engineering, Faculty of Civil Engineering and Geosciences, Delft University of Technology, Delft, The Netherlands
[2] Hydraulic Engineering, Deltares, Delft, The Netherlands
[3] Laboratory for Aero & Hydrodynamics, Faculty of Mechanical Engineering, Delft University of Technology, Delft, The Netherlands

E-mail: w.bakker-3@tudelft.nl

Received 16 April 2021, revised 13 July 2021
Accepted for publication 26 July 2021
Published 16 August 2021

Abstract

In this paper the development of a high-power pulsed LED line light and its use to apply particle image velocimetry (PIV) during wave impact measurements are described. An electrical circuit that generates high-current pulses is designed and built, which is used to overdrive a number of commercially available LEDs. The limit for this overdrive-capacity is determined as function of pulse duration for various commercial available LEDs. Two systems of cylindrical convex lenses are designed to act as a collimator and reduce divergence of the LED bundle and the resulting light sheet properties (maximum light intensity and sheet thickness) are investigated. An array of LEDs of 60 cm length (referred to as the *LED line light*) is designed and manufactured. For the two lens systems, the LED line light provides proper light sheet conditions to illuminate measurement regions in the order of either 0.3×0.3 m^2, or 1×1 m^2, at a sufficiently constant light sheet thickness of 5 mm. The application of the LED line light is demonstrated by quantifying the instantaneous flow field of a wave impacting on a blunt object in a wave flume. PIV measurements are conducted at an acquisition rate of 25 frame pairs per second, quantifying maximum flow velocities in the order of 1.0 m s^{-1} at a LED pulse width of 200 μs. The system, consisting of the LED line light, a CMOS camera and open source PIV processing software provides the possibility to perform 2D planar PIV measurements for a fraction of the costs of a commercially available laser based PIV system.

Keywords: LED line light, particle image velocimetry, large-scale PIV, LEDPIV, wave load, wave impact

(Some figures may appear in colour only in the online journal)

* Author to whom any correspondence should be addressed.

1. Introduction

Particle image velocimetry (PIV) is a measurement technique in fluid mechanics to instantaneously quantify a flow at high resolution by determining the displacement of a large number of particles that are assumed to follow the flow. A PIV setup consists of five components: (a) a flow seeded with tracer particles; (b) a light source to illuminate the particles; (c) one or multiple cameras to image the location of the particles; (d) a timing unit to synchronize camera's and light source and (e) a system to store the images. The majority of PIV measurements are performed with the use of commercially available laser-based systems, which are developed to enable a wide variety of PIV measurements (planar, stereo, volumetric and tomographic PIV). However, to apply the basic form of PIV known as *planar PIV*—which is widely applied in academic research and industry—a more simplistic system suffices. This paper presents an alternative, user-friendly system to conduct PIV measurements in large scale, industrial surroundings, focussing predominantly on an alternative type of light source.

The majority of PIV experiments are conducted with a (pulsed or continuous) laser as source of illumination [1, 2]. Lasers emit collimated and coherent light, providing excellent light sheet properties over a large distance from the laser head. Furthermore lasers are capable of generating high intensity nanoseconds pulsed light beams, which enables the illumination of fast moving tracer particles while preventing image blur [3], thereby providing the possibility to quantify high velocity flows. However, the application of lasers brings along the disadvantage of strict laser safety precautions, which can form a serious drawback for PIV measurements in large experimental setups [4]. In addition to that, the intensity distribution of a laser sheet formed by spreading of a laser beam into large measurement regions ($>1 \times 1$ m^2) has found to be inhomogeneous over its width and can result in partly shadowing of the measurement area. Moreover, it limits the possible size of the illuminated area. A pulsed PIV laser consists of multiple (in most cases two) laser cavities, which can cause large measurement errors in case of misalignment or improper overlap [5]. Furthermore, pulsed high power laser systems are complex, expensive and vulnerable for contaminations present in and around the experimental setup. Concluding, lasers have disadvantages regarding safety, complexity, large field-of-views and the systems are expensive. For these reasons, studying the use of alternative light sources for large scale (1×1 m^2) PIV measurements (i.e. light sources other than (pulsed) lasers) in hydraulic applications is of interest.

A widely studied alternative is the use of light emitting diodes (LEDs). Recent developments in LED manufacturing resulted in an increased light output and life span while reducing the costs through mass production. Other than lasers, LEDs generate uncollimated, incoherent light, giving much lower radiation levels (amount of radiant flux per unit of surface area), appearingly, making them less applicable in planar PIV applications. However, LED bundles can be collimated applying lens arrays [6, 7], resulting in a strong decrease of the divergence angle and thereby significantly increasing the luminosity at large distances from the light source. On the other hand, this can form an increased risk of eye (and skin) damage. The lens of a human eye focusses light to a spot on the retina, which can result in permanent blindness in case of high irradiance levels. Collimated, coherent laser light can be hazardous at relatively low exposure levels, while LEDs (even in combination with a collimator) distribute the exposed light over a larger spot on the retina, resulting in lower retinal irradiance [8, 9], making LEDs a less eye-hazardous alternative as illumination source than lasers. Furthermore the emitted radiance of a pulsed laser (typically in the order of 1–10 MW for nanosecond pulse widths, with all radiation bundled in a small beam) is orders of magnitude larger than that of an LED [4, 10].

Previous studies show successful application of single LEDs as illumination source in micro-PIV [11–14], tomographic/volumetric PIV [15–17], Schlieren imaging [18] and particle-shadow velocimetry [19]. The ability of LEDs to be overdriven using short duration pulses with currents much higher than prescribed by the manufacturer is described and applied to small scale (50×50 mm^2) PIV measurements both in air and water (velocities up to 0.5 m s^{-1}) [10]. In addition to these studies with single LEDs as light sources, the application of LED light arrays have been investigated as well. The water flow around a grid of cylinders was characterized through a region of 0.5×0.5 m^2 [20]. This study shows promising results, however the LED line light is not well described and the light source only provides light conditions to quantify relatively low flow velocities (maximum of 25 cm s^{-1}). Furthermore, PIV measurements in a pump sump have been conducted for velocities up to 4 m s^{-1}. This was implemented with a commercially available PIV system and LED line light, which could not be overdriven and therefore was experiencing strong image blur [4]. LEDs are recognized as an alternative for lasers, however the mentioned studies focus on small scale flows of relatively low velocities, which can be considered as the main challenges for application in large-scale industrial surroundings.

This work presents an in-house developed LED line light which is used as illumination source to conduct PIV measurements. The technical details of the components and the properties of the emitted light sheet are described and the application of the light source in combination with a low-cost CMOS camera and PIV processing software is presented. Instantaneous data and velocity fields of an impact of a wave on an overhang are shown.

2. LED line light development

Ultimately the developed LED line light is able to generate a pulsed, high intensity light sheet in the order of 1×1 m^2, with a light sheet thickness (Δz) in the range of 1–5 mm. Firstly a number of LEDs is tested on its pulsed overdriving capacities. Secondly an optical system is designed to collimate the diverging LED bundle, resulting in a sufficiently thin light sheet. Finally the characteristics of the light sheet are measured and compared with a commercially available LED line light.

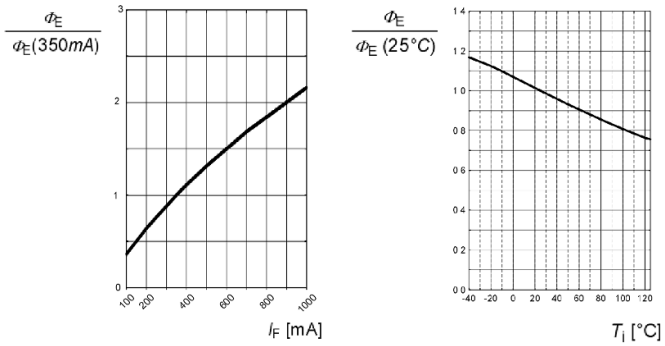

Figure 1. Response of LED characteristics due to overdriving (increase of forward current) in continuous mode, which shows an increase in luminosity for an increase in forward current (left), but a decreasing luminosity for increasing LED temperature (right), where Φ_E = luminous flux (lm), I_F is forward current and T_j is junction temperature (redrawn from Osram LED datasheet).

2.1. High-power operation

Overdriving of LEDs is defined as an increase in the voltage (V_p) that is applied to the LEDs. Commonly LEDs are used for continuous illumination and therefore manufacturers will provide data on their performance under such conditions. As can be observed in figure 1, the relative luminous flux that is emitted by this LED increases proportional to the increase in applied voltage, resulting in an increase in current. However, high levels of overdriving cause an increase in internal temperature of the LED, negatively effecting its efficiency and decreasing its luminous flux. Furthermore the lifetime of LEDs strongly reduces by intense overdriving, eventually leading to breakdown of the LEDs [10].

To determine the type of LED that will be used in the line light design, a number of different LED types are tested on their overdriving capabilities in pulsed operation. Strong, pulsed overdriving gives high radiation for a short period of time, which is essential for the desired PIV applications. According to optical theory [21], a modest luminescent area of the LED is desired, since collimation of small light sources is more effective, which simplifies the formation of a thin light sheet. Furthermore all LEDs emit green light (λ_{peak} = 520–560 nm), which is advantageous since most camera chips that are used for PIV applications are most sensitive to this wavelength band. Moreover, in water green light attenuates much less than red light [22].

An electrical circuit was designed (based on the driver circuit used in [10]) consisting of a low and high voltage part, to generate short duration, high current pulses. The high voltage part (see figure 2) is fed by a 120 volt DC power supply (IN2). The low voltage circuit generates a pulse (IN1) which shape can be optimized using potentiometer P1, which is the input of the FET's gate. Energy to power the LEDs is stored in the pair of electrolytic capacitors (C8/C9 and C10/C11), where the charging of capacitor pair C8 and C9 (with a capacity of 2200 μF and 100 nF respectively) is set by resistance R13. The LED is protected against reverse currents by diode D2 and the input current is obtained from the voltage measured over resistance R12.

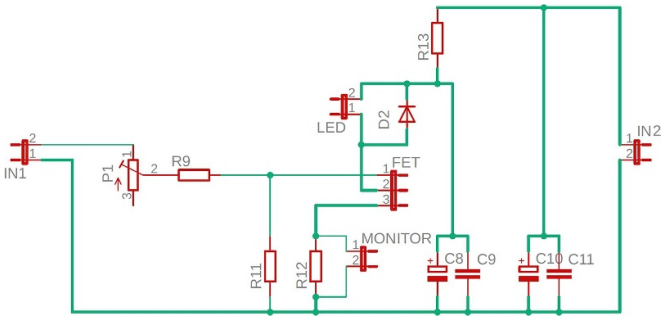

Figure 2. Schematic representation of electrical circuit to generate high current pulse to overdrive LEDs.

The properties of the tested LEDs are given in table 1. These LEDs are connected in series and are driven with current pulses varying in pulse duration (τ_p) and current (I_p). Next, the pulsed current damage threshold is obtained, either by increasing the pulse width, or the current, up to the breakdown of the LEDs.

The different LEDs are tested on their overdriving capabilities for a relatively short pulse duration of $\tau_p = 7.5$ μs. A small value of the pulse width reduces the chance of motion blur of an imaged particle that is illuminated for the envisaged hydraulic applications. All LED overdriving tests described here were performed for a 20 Hz pulsed current. The forward voltage and the number of LEDs in series can be adapted, such that the current level varies. The results of the tests are shown in figure 3. In the left plot, the overdriving capabilities of the four LEDs are shown for $\tau_p = 7.5$ μs. All types of LEDs can be overdriven up to current levels 15 to 100 times larger than in continuous mode (see $I_{p,cw}$ in table 1).

From the results in figure 3 and the properties listed in table 1 it is concluded that the Osram Oslon SSL80 shows best performance to apply in the LED line light. For varying pulse widths, the damage threshold of the Osram LED is shown (right graph of figure 3). As can be observed, the pulsed current damage threshold decreases logarithmically with the pulse width. This result corresponds to the findings in literature [10] and provides the possibility to determine the maximum permissible pulsed current such that operational damage is prevented. It is expected that overdriving the LEDs at relatively high pulse widths ($\sim\tau_p = 1$ ms) will negatively influence the lifetime. However, when the lifetime of an LED operating at 10% duty cycle due to this overdriving is reduced by a factor of 100 (as compared to the LEDs lifetime of 100 000 h under continuous operation and nomimal voltage) it is still comparable to a pulsed PIV laser (generally with lamp lifes of 1×10^7 pulses). The electrical system that generates the high current pulses was adapted to prevent this limit to be exceeded accidentally, by the addition of a resistance (R13 = 680 Ω in figure 2), that decreases the maximum amplitude of the pulsed current for increasing pulse widths.

2.2. Optics

Unlike laser beams, light generated by LED light sources is strongly diverging (see the values of θ in table 1, such that

Table 1. Properties (in continuous work mode) from datasheet of LEDs used for overdriving capability test. $I_{p,cw}$ = current in continuous mode,V_f = forward voltage at nomimal current ($I_{p,cw}$), A_{LED} = LED's radiating area, θ = the divergence angle of the LED bundle, λ_{peak} = wavelength of maximum luminous radiation and K = luminous efficacy.

LED type	$I_{p,cw}$ (A)	V_f (V)	A_{LED} (mm^2)	θ (°)	λ_{peak} (nm)	K (lm W^{-1})
Nichia NF2W757DRT-V1	0.4	7.0	3 × 3	120	540	107
Osram Oslon SSL80	0.35	3.3	3 × 3	80	521	111
Lumileds LXML-PM01	1.0	2.9	3.7 × 4.6	120	530	101
Seoul Semicond. G42180	0.35	3.3	7.4 × 7.4	130	525	70

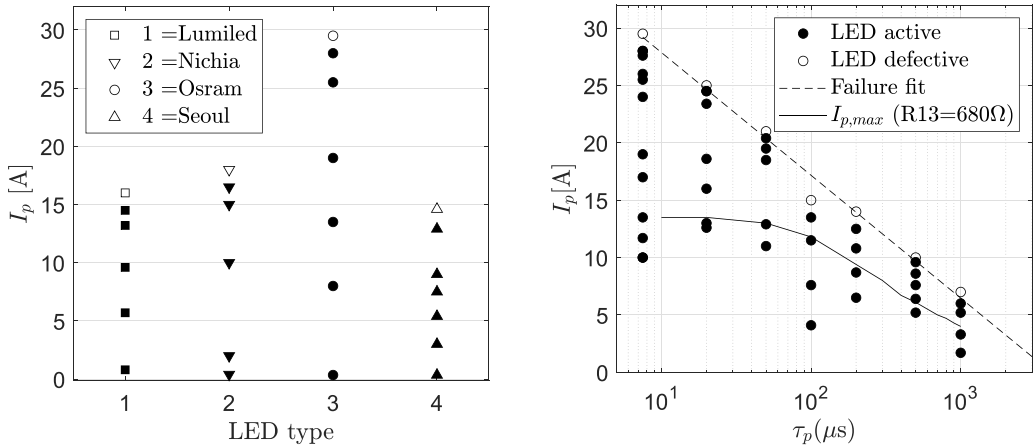

Figure 3. Response of LEDs on overdriving (increase of forward current); different types of LED in pulsed mode for $\tau_p = 7.5$ µs (left, where unfilled markers indicate the breakdown of the LED) and overdriving capability of Osram LED for varying pulse widths (right).

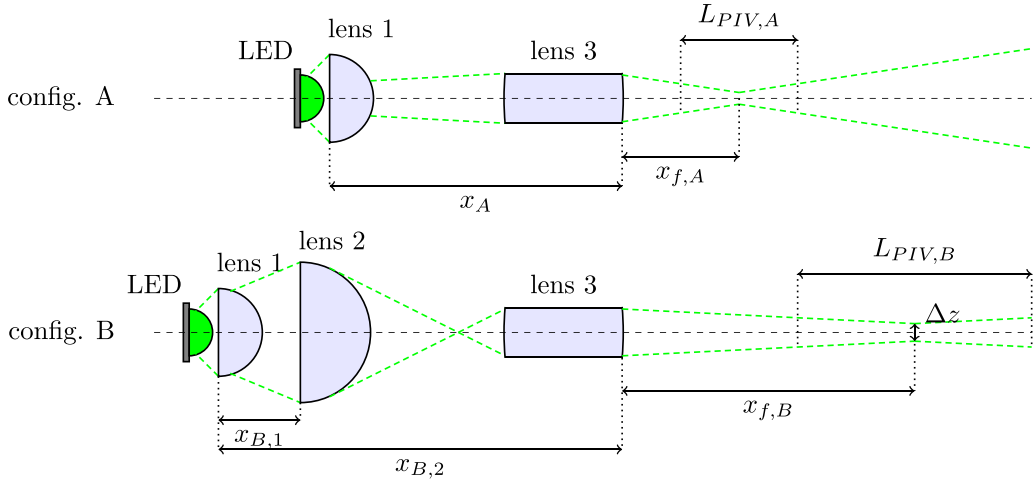

Figure 4. Schematized sideview of LED light sheet for the two different lens configurations, with the following lens properties: lens 1: plano-convex cylinder, with radius of curvature (r) = 5 mm, lens 2: plano-convex cylinder, with r = 10 mm and lens 3: bi-convex cylinder of 20 mm height and 100 mm wide, with r = 135 mm. All lenses are made from PMMA, which has a refractive index of ∼1.49. Lenses 1 and 2 are commercially available standard material and lens 3 was custom made and designed particularly for this purpose.

the illuminated volume strongly increases with distance form the LED. This characteristic makes the application of LEDs as illumination sources for PIV measurements undesirable. By application of a system of convex lenses, the diverging bundle can be collimated, forming a thin light sheet. The light sheet properties depend on the position and radii of curvature of the lenses. Due to the LEDs not being point sources, basic optical theory (such as the thin lens formula [21]), appeared not to be applicable to the situation. Therefore a number of different configurations (either with two or three lenses) were tested for their ability to decrease the light sheet thickness and increase its luminosity (see figure 4).

Light is generated by an array of 120 mm in length, containing 15 LEDs which are connected in series and are mounted with an underlying distance of 8 mm. Starting point was a lens with large radius that had shown to act as proper LED collimator in a previous study [4], in which the distance between the LEDs and lens was relatively large resulting in loss of large

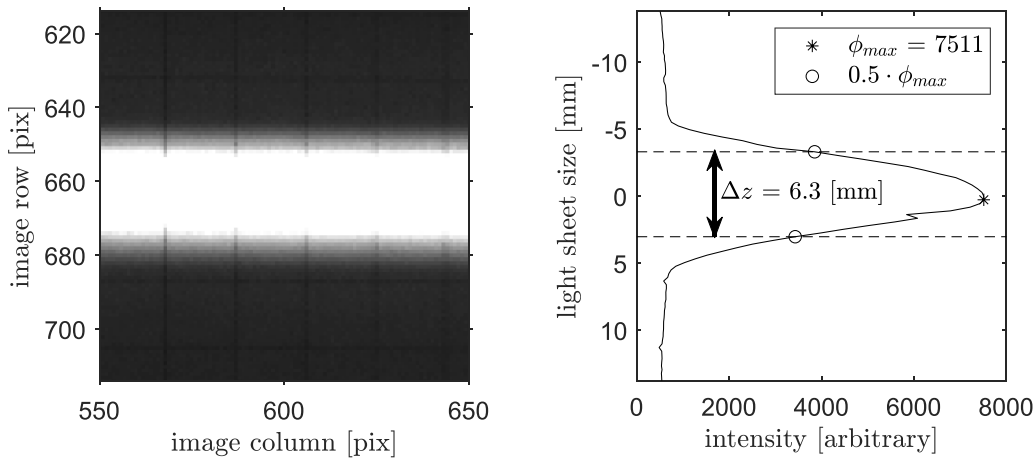

Figure 5. Measuring LED light sheet properties, left: part of image of the reflected light sheet, right: intensity peak (average of 100 pixel columns) over image height and derived light sheet thickness Δz.

part of the LED bundle. By placing an additional collimating lens close to the LED, this loss was thought to be decreased. Changing positions and radii of curvature of the lenses resulted in a wide variety of light sheet conditions. For certain lens configurations no collimation is achieved, however by applying the Lensmaker's equation [21] lens configurations estimates are found. The combination of a relatively large angle of divergence of the LED and a desired large focal length of the optical system, results in large loss of the LED output. The majority of the loss occurs at lens 3, which (using the Lensmaker's formula and the lens properties as stated in the caption of figure 4) has a focal length of approximately 700 mm and thus a very small aperture. Lenses 1 and 2 on the other hand have an estimated focal length of 10 and 20 mm respectively and will therefore cause muss less light loss.

By an additional trial-and-error approach a converging light sheet was obtained, up to a point where the light sheet thickness reaches its minimum (referred to as the focal point x_f). From that point onwards the light sheet is diverging (see figure 4). The distance over which the light sheet is sufficiently thin to conduct PIV measurements is defined as L_{PIV}. Along this distance it is demanded that $\Delta z \lesssim 5$ mm, for interrogation window sizes in the order of 10 mm to ensure cubic sampling volumes [23]. Note, that all lenses applied in this study are cylindrical, therefore the LED bundles are collimated in one direction only.

2.3. Light sheet characteristics

In order to compare the effect of the different lens configurations, the intensity of emitted light is quantified with a CCD chip, by capturing the reflections of the light sheet radiating from a white opaque surface (i.e. the illuminance at this surface), keeping its distance to the CCD fixed. Each row of pixels of the chip is averaged over one hundred columns along the centre, resulting in an intensity distribution over the height of the chip (see figure 5). Pixel distance is converted into meters with the grid lines at white surface reflecting the emitted light. The LED array consists of 15 LEDs at an underlying distance of 8 mm, that are (SMD) soldered on a printed circuit board (PCB). To ensure a longer lifetime, the LED arrays are mounted on an aluminium extruded heat sink profile in combination with thermal paste to increase heat dissipation. The distance between the LEDs and first lens is fixed ($\sim$2 mm) by a number of spacers, providing support to the first lens.

The performance of the LED line light is expressed by the maximum illuminance (ϕ_{max}) and the thickness of the light-sheet (Δz) as a function of the distance from the lens furthest away from the LED array (i.e. lens 3 in figure 4). The thickness of the lightsheet is defined as the full width at half of the maximum intensity (FWHM, which is the distance between the values closest to $0.5 \cdot \phi_{\mathrm{max}}$ on both sides of the intensity peak, see right part of figure 5).

Depending on the demands of the measurement where the LED line light is applied, a specific lens configuration can be chosen. In case a relatively large measurement plane is required—say for PIV measurements of 1×1 m^2—the configuration with three lenses (bottom part of figure 4) is recommended (as can be observed from the results in figure 6). This configuration provides modest convergence and divergence and thus a thin light sheet over a large distance from the lens system (represented by a large value of L_{PIV}). However, for measurements closer to the LED line light the two-lens configurations performs better, with a high intensity and thin light sheet as can be observed in figure 6. The performance of the LED line light with the two different lens configurations is compared with that of a commercially available alternative (DrewLear VLX2-500, $\lambda_{\mathrm{peak}} = 528$ nm), in combination with a biconvex cylindrical lens to adapt the light sheet characteristics used in [4]. The results are shown in figure 6. The intensities of the newly developed line light are significantly higher, even for the short pulse duration cases (not shown). The maximum intensity of the developed line light is more than an order of magnitude higher than the commercially available line light for the same exposure time, due to the applied overdriving. On the other hand, the minimum light sheet thickness is smallest for the DrewLear line light. However, the variation of the light sheet thickness over the distance from the lens is much smaller

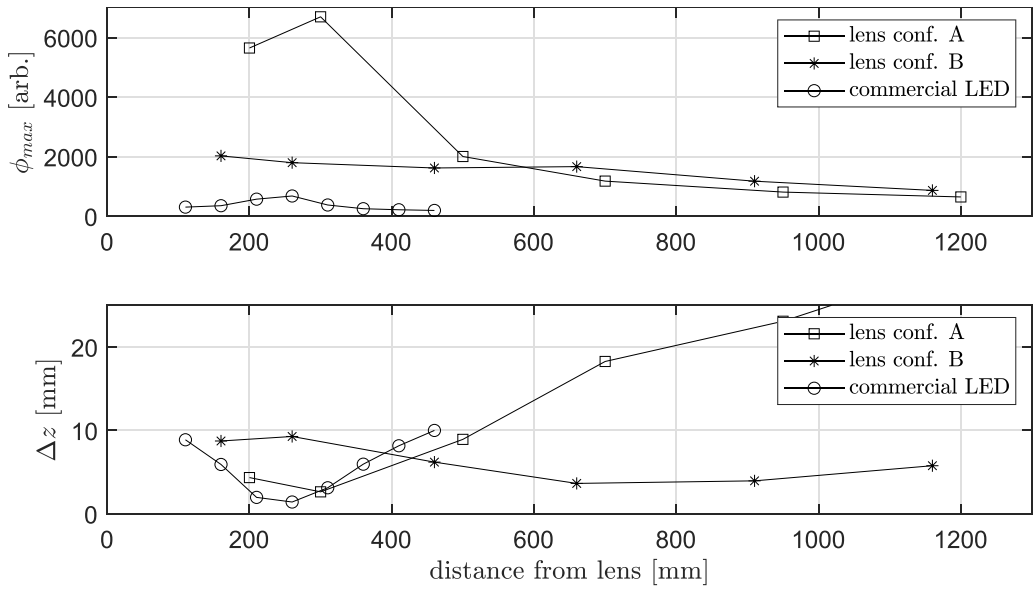

Figure 6. Light sheet properties for different lens configurations, compared with commercially available line light system: maximum light intensity (top) and light sheet thickness (bottom) as a function of the distance from the LED's lens (all data obtained for $\tau_p = 100$ µs and $I_p = 10$ (A).

Table 2. Properties of LED line light sheet for different lens configurations, variables as defined in figure 4.

Lens conf.	x_{lens} (mm)		x_f (mm)	L_{PIV} (mm) ($\Delta z \leqslant 6$ mm)
A	$x_A = 250$		300	∼250
B	$x_{B,1} = 95$	$x_{B,2} = 340$	800	∼800

for lens configuration B. This variation (represented by L_{PIV}) is an important parameter, since a varying light sheet thickness can have a negative effect on the accuracy of a PIV measurement [23]. Note that both the DrewLear line light and newly developed line light with lens configuration A are designed for much shorter working distances, while the line light with lens configuration B shows better characteristics for large working distance conditions.

A way to limit the thickness of the light sheet introduced by [20] is through the use of a slit in front of the last lens, such that the outer part of the light sheet is blocked. However, this result could not be reproduced. The variation of the luminosity along the length of the LED array is not quantified, it is however expected that this variation is very small since a large number of LED bundles is overlapping along the -uncollimated- length of the LED array. Furthermore, the main part of the luminosity of each LED bundle radiates along the centre of the light bundle, resulting in a high intensity light sheet with a length similar to the length of the LED array.

The influence of the pulse width and forward current on the luminosity ϕ are investigated in the same test setup as is described at the beginning of this section, the results can be observed in figure 7. The luminosity of the LEDs scales linearly with the exposure time, as expected. Furthermore, the luminosity scales non-linearly with the input power ($P_p = V_p \cdot I_p$), which corresponds to the behaviour observed in figure 1, where the luminosity of the LED shows a non-linear trend with forward current. Furthermore, from the LEDs datasheet it is obtained that the forward voltage is not proportional to the applied current, contributing to the non-linear relation between P_p and ϕ. Especially for large values of P_p the increase in luminosity is limited, which is thought to be an indication of the negative influence of temperature rise on the luminous efficacy of the LEDs (see figure 1). However, the drop in luminosity is not significant and a linear relation with the electric energy input ($E_p = P_p \cdot \tau_p$) is found.

Generally speaking, the LED line light can be applied for planar PIV measurement of a region that has dimensions of L_{PIV} by L_{PIV} and its center is located at x_f from the LED unit. The length of the LED line light (which defines the height or length of the illuminated region) and its lens configuration can be chosen, such that the desired light sheet properties are met (see table 2).

3. Application of LED line light in wave load measurements

The high-pulsed LED line light as described in the previous sections is used as an illumination source for a number of PIV measurements in a wave flume. The objective of the measurements is to obtain the two-dimensional (direction of wave propagation and normal) velocity field of the water flow prior to and after a wave impact on a blunt object with an overhang.

3.1. Experimental setup

The experiments are conducted in a wave flume at the Hydraulic Engineering Laboratory at Delft University of

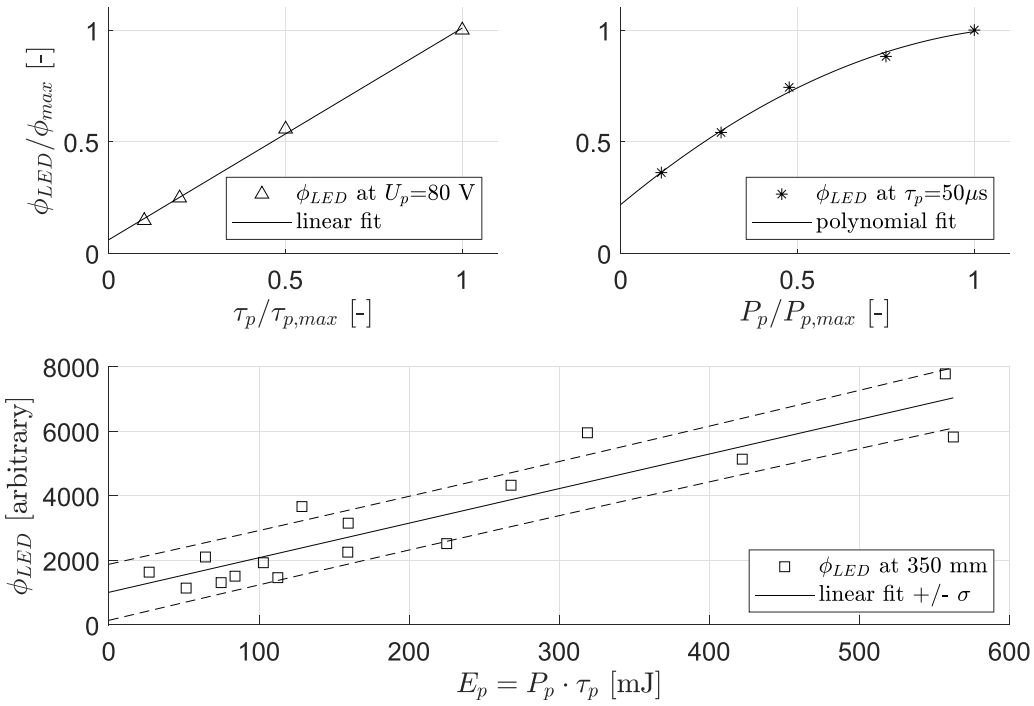

Figure 7. Luminosity of LED line light with lens configuration A measured at 35 cm from lens 3, under varying pulse durations and forward currents, pulsed at $f_p = 20$ Hz.

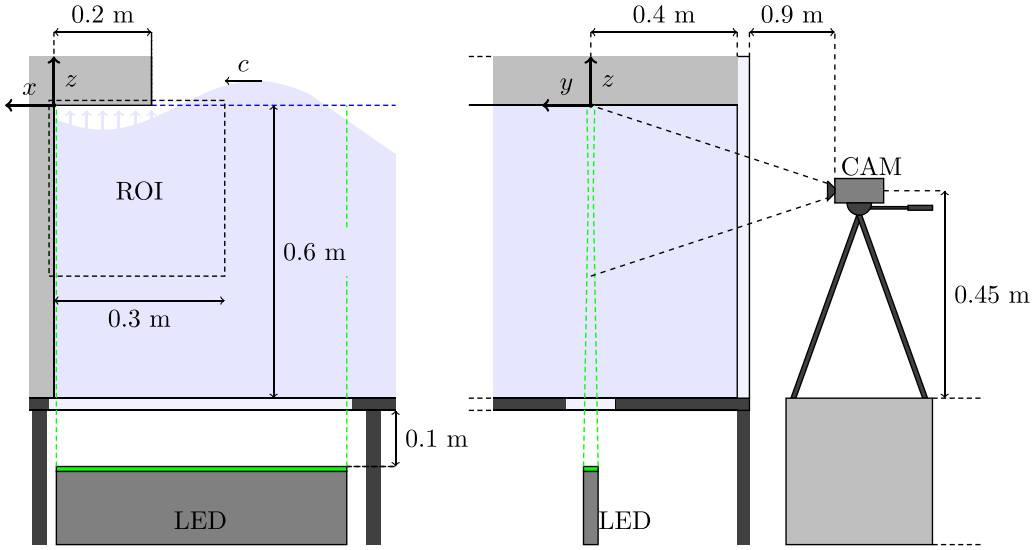

Figure 8. Sketch of experimental setup of wave-impact measurements (not to scale), from camera point of view (left) and as seen from the downstream side of the flume (right). ROI = region of interest, c indicates the direction of the wave propagation.

Technology. The flume has an effective length of 39 m and a width of 0.80 m. Waves are generated by a hydraulically driven wave generator with active reflection compensation. The setup is illustrated in figure 8.

For a description of the entire setup the reader is referred to [24]. A concrete block with an aluminium construction representing an overhang (of 0.2 m long, at 0.6 m from the flume bottom) is placed at 23.3 m from the wave generator. The side walls are 1.5 m wide glass windows -providing optical access-, supported by a metal construction. A CMOS camera (FLIR Oryx 2448 $\times$ 2048 pix^2 chip, pixel size $d_\tau = 3.45$ µm, 8 bit dynamic range), with a 28 mm lens (Nikon Nikkor 28 mm f/2.8 Al-s with focal ratio $f^\# =$ f/5.6) is positioned perpendicular to the side wall. The distance between the camera's chip and the flume's side wall is 0.9 m, providing a field of view of approximately 0.4 m by 0.35 m, such that the impact region is imaged in detail. The LED line light (which is 0.6 m long and consists of 5 PCB's connected parallel, each with an array of 15 LEDs) is placed below the wave flume at the location where a 0.8 m long and 0.2 m wide glass slit is installed in the flume bottom, which enables the light sheet to access and illuminate the measurement region. The

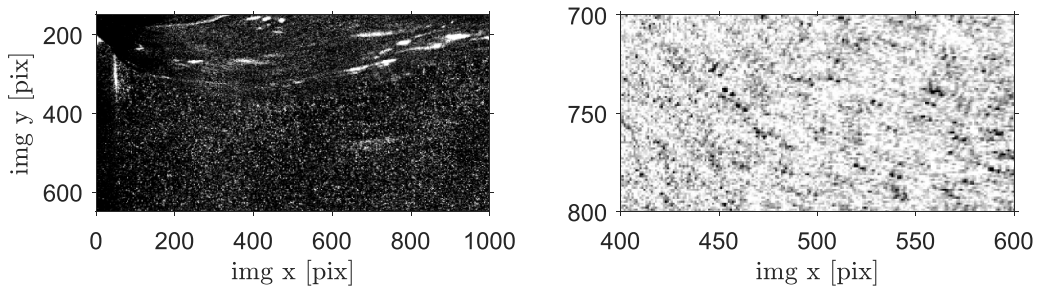

Figure 9. Section of unprocessed images used for PIV analysis. Left: single instantaneous image of illuminated particles and free surface located below overhang, with the vertical wall visible on the left; Right: inverted image of frame pair (sum of two frames), showing particle displacement during Δt of a region of the flow below the region shown in the left figure.

wave flume is seeded with tracer particles (Vestosint 1101, $\rho_p = 1060\ \mathrm{kg\,m^{-3}}, d_p = 100\ \mu\mathrm{m}$). Part of the flume is covered with shielding material to block ambient light and also preventing direct exposure of the LED to people in the vicinity of the measurement area. Note that in case a laser was used much stricter safety precautions should have been taken, (i.e. shielding of the complete flume with laser safe material), which is a tedious and expensive execution.

Lens configuration B is applied in all the experiments, since this configuration provides a sufficiently thin light sheet at the impact region. The camera and LED are triggered by a pulse generated by the software provided by the manufacturer at 50 Hz (SpinView) and the delay to trigger the LED varies between the frames of each frame pair, such that the first frame is illuminated at the end of the exposure, while the second frame is illuminated at the beginning, which is known as *frame straddling* [3]. This enables a sufficiently small Δt (100–500 μs) to obtain particle displacements satisfying the PIV design rules [1] during the measurement. Images are written to an SSD drive on a local PC and are post-processed using the open source freeware OpenPIV [25].

3.2. Instantaneous results

The results presented in this work are based on one particular wave case, while interest lies in demonstrating the applicability of the measurement technique and validating its accuracy, rather than examining or understanding the fluid mechanics (which are described in more detail in [24]). The PIV analysis presented here is based on a series of regular waves ($T = 1.3$ s, $H = 0.06$ m, corresponding to case A60L in [24]) impacting on a 0.2 m long overhang, which is located at the same height as the mean water level, which is 0.6 m from the flume bottom (see figure 8).

A measurement series consists of 2000 images, acquired at 50 frames per second, corresponding to 1000 PIV vector fields obtained at 25 Hz. To enable a sufficient pixel displacement of the particles through the complete region of interest, the time-delay is set at $\Delta t = 4500$ μs. The pulse width is set at 200 μs, providing sufficient contrast between illuminated particles and the background, while avoiding image blur, which may occur for large pulse widths at high velocities [3, 4]. From the unprocessed data (see figure 9) it is obtained that the particle image diameter is 2–3 pixels.

As can be observed in the image of the wave impact (see figure 10), a considerable part of the measurement area shows the air above the free-surface. Which -in addition with reflections of the LED on the free-surface- prevents the possibility of background subtraction as preprocessing step. It was found that illuminated particle's intensity is in the order of 50 greycounts as compared to the background's intensity of 10 greycounts, which was found to give consistent instantaneous vector fields. Distortion of the images are corrected by applying the intrinsic calibration parameters as obtained with the camera calibration application in Matlab [26]. The undistorted frame pairs are processed with PIVlab 2.31 [25], with rectangular interrogation window size $D_I = 128$ pix and 50% overlap, results in a vector resolution of 10 mm. A local median filter [27] is applied (threshold = 2, epsilon = 0.1) to detect and filter outliers, finally missing data is interpolated. From visual observation of the raw images, motion blur seems limited. This is supported by the analysis of the pixel displacement data -which shows no peak locking- and the number of rejected vectors being in the order of 1%–2% of the total number of vectors, giving confidence in the quality of the acquired images. In case a second interrogation step with $D_I = 64$ pix is applied, the percentage of rejected vectors slightly increases, but remains below 5% of the total vectors. A set of instantaneous vector field prior to and after a wave impact is shown in figure 10. As can be seen, the experimental method is able to quantify the rapidly varying flow phenomena that take place during a wave impact.

3.3. Comparison with wave gauge measurement

To get an indication of the accuracy of the performed PIV measurements, the obtained vertical velocities along the wall (at $x = -0.005$ m) are compared with the velocity of the free surface at the vertical object, which is derived from a wave gauge signal (see figure 11). The wave gauge is flush-mounted along the height of the vertical object, close to the centre of the flume. The wave gauge signal is filtered at 10 Hz to reduce the effect of noise in the derivation of the velocity. The position of the free surface as measured by the wave gauge corresponds well with visual inspection of the free surface location from the PIV images (see top part of figure 11), which partly confirms the timing of the pulsed light sheet.

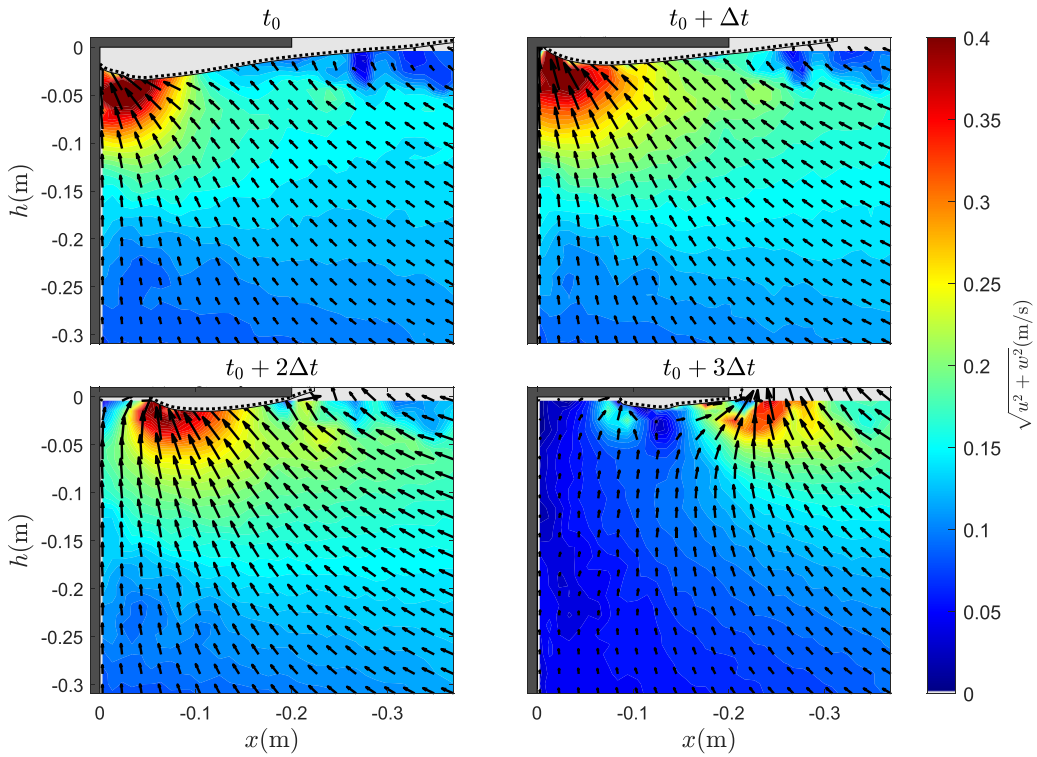

Figure 10. Sequential velocity fields (every second vector is shown) of wave impacting on a vertical object (on the left side of the figure) with an overhang. Prior to the wave impact (top left and right, and bottom left) and after wave impact (bottom right) when the flow settles. The dotted lines represent the free surface and region above it (light gray) is masked out.

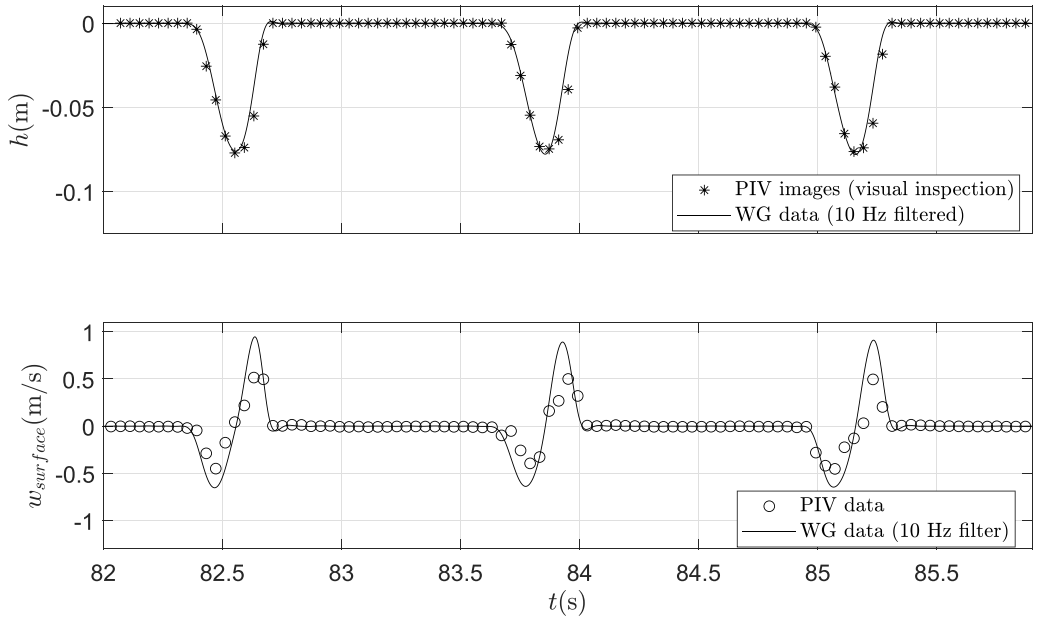

Figure 11. Bottom plot shows comparison of instantaneous vertical velocity component at the wall (below the overhang) as obtained from the wave gauge (WG) measurement and PIV analysis. The PIV data plotted is obtained at the location closest below the free surface position, as measured by wave gauge (shown in the top part of the figure).

The vertical velocity of the PIV analysis is given at the location of the free surface obtained from the wave gauge. Signal acquisition of the instruments is synchronized in time. The results do not show any phase-shift between the two measurement techniques and the magnitude of the vertical velocities show acceptable resemblance. Significant differences are observed at the positive and negative peaks of the velocity signals, where the velocities derived from the wave gauge signals are approximately 30%–40% higher than the magnitude obtained with the PIV analysis. PIV can give inaccurate results for flows

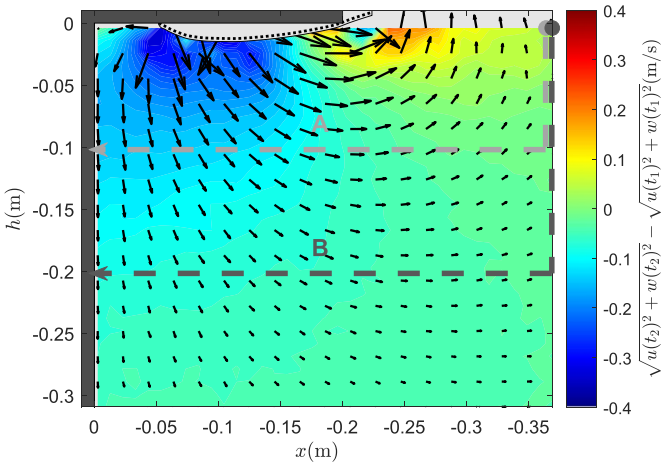

Figure 12. Vector field of velocity difference between two subsequent instantaneous velocity fields (bottom left and right contourplot in figure 10) and integration paths that are followed for the analysis shown in figure 13. Note that t_1 and t_2 are respectively equal to $t_0 + 2\Delta t$ and $t_0 + 3\Delta t$ in figure 10.

close to a wall due to insufficient resolution of the interrogation windows [28]. Interrogation refinement along the walls can possibly reduce the error. Furthermore PIV is known for its velocity bias towards smaller values due to underestimation of the correlation values at large displacements [29]. And from the raw images it is observed that the free surface is strongly reflecting the LED light, which are thought to increase the inaccuracy of the PIV results [30]. It should be noted that the deviation in velocity quantification is expected not to be caused by the type of illumination.

3.4. Pressure-impulse from PIV velocity field measurements

The PIV velocity field measurements before and after a wave impact were also used for estimating the given wave impact pressure-impulse (i.e. the area enclosed by the pressure-time curve between impact start and impact end). From the velocity change field ($\Delta\vec{u} = \partial\vec{u}/\partial t = \vec{u}(t_2) - \vec{u}(t_1)$) evaluated from the wave impact shown in bottom left and bottom right plot in figure 10, the pressure-impulse (∇P) is estimated according to $\nabla P = -\rho\partial\vec{u}/\partial t$ (see [24] for the derivation of this expression), where P [Pa] is the pressure and ρ (kg m^{-3}) is the fluid density. The integration of P was carried out starting from the top right location in the vector field, which is close to the free surface position, such that we may assume $P = 0$ and following two different integration paths (A and B) shown in figure 12.

The pressure-impulse obtained with this method at the vertical wall was compared with the pressure-impulse measured by pressure sensors located at 4 locations at the vertical wall (0.02 m, 039 m, 0.55 m and 0.59 m.), see figure 13. The comparison between the two methods is shown in the right hand side of figure 13, where a close agreement is found. At the top of the vertical wall (i.e. where the horizontal overhang is located), discrepancies between the two methods are stronger. A main reason for these discrepancies is the presence of air pockets below the overhang during wave impacts, which was studied in more detail by [31].

4. Discussion

The results presented in the previous sections show that the in-house developed LED line light can act as an illumination source for large-scale planar PIV measurements. The use of LEDs as an alternative for conventional laser-based illumination brings along a number of challenges, such as the relative low luminosity and highly diverging LED light bundle.

These measurements are conducted with a field-of-view of approximately 30 $\times$ 30 cm^2, however the area of interest can be increased significantly. With this particular line light, an area of 0.6 $\times$ 0.6 m^2 can be illuminated homogeneously, while this area can be increased for a longer LED line light.

In this work the luminosity of the LEDs is increased by steering the LEDs with much higher pulsed currents than is applicable in continuous mode. This approach can increase LED luminosity up to a factor 40 for low duty cycles (ratio between pulse width and time-instance between two pulses), which is typical for PIV measurements in hydraulic engineering applications. However for higher duty cycles the increase in luminosity is more modest to prevent thermal damage of the LED. The present study is represented by a low duty cycle, with pulse width $\mathcal{O}$ (100 µs) allows good PIV measurements of flow velocities of $\mathcal{O}$ (1 m s^{-1}). Furthermore, relatively large pulse widths can induce motion blur of the imaged particles, which can result in a decreasing accuracy of the PIV analysis. An increase in luminous efficacy in LED development can overcome these challenges.

The LEDs are collimated with a system of convex cylindrical lenses, which -in the presented configuration- gives appropriate light sheet properties, but results in a significant loss of light. A more efficient way of collimation could be achieved by the use of complex lenses, such as GRIN-, or Fresnel lenses [32] or 3D-printed lenses designed with the use of ray tracing software. In addition to that, an increase in the luminous efficacy will result in smaller radiating surface of LEDS, providing more effective collimation. On the other hand, the fact that the light sheet diverges after the focal point can also be interpreted as an advantage in the light of eye-safety. The increase in light sheet thickness goes hand in hand with the decrease of the luminosity. So for the application in large-scale industrial facilities (where laser-based illumination can become problematic), people standing outside the near vicinity will be exposed to low, unharmful emission levels. Additional measurements in which the luminosity (or ideally the photometric irradiance) of a LED line light is compared to that of a conventional laser light sheet would be very helpful. Such measurements can give a better indication for the application range (flow velocities) under which a LED line light can be applied as light source for PIV measurements.

As is demonstrated, the light sheet properties can be adapted by choosing the appropriate lens configuration and size of the LED line light. The current design provides the possibility to conduct PIV measurements of moderate flow velocities

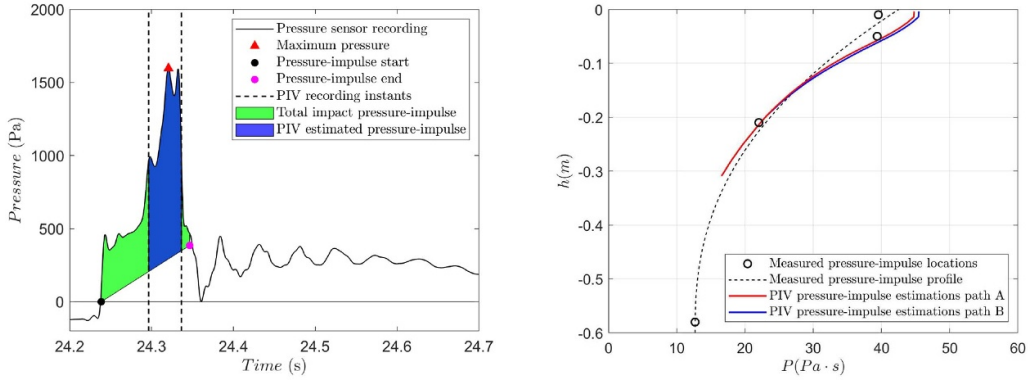

Figure 13. Comparison between two methods for estimating the pressure-impulse at the vertical wall during a wave impact: from pressure measurements and from velocity change measurements with LEDPIV. Left: Signal from pressure sensor during wave impact, with instants of acquisition of PIV frame pairs. For clarity the PIV recordings instants are plotted as (dashed) lines, while in reality they posses a finite width equal to Δt Right: Comparison between the two methods, including two integration paths in the velocity change field (as displayed in figure 12). The vertical dashed lines represent the integration limits for pressure to determine the pressure impulse, $t_1 = t_0 + 2\Delta t$ and $t_2 = t_0 + 3\Delta t$, which are equal to the times that the velocity fields were recorded to determine Δu.

$\mathcal{O}$ (1 m s^{-1}) (preventing image blur) in regions up to 1 $\times$ 1 m^2. With future improvements of the optics and increase of the luminous output of the LEDs, larger domains, higher flow velocities and more turbulent flows (shorter pulse widths provides higher frame rates) can be quantified. An alternative application of high-power pulsed LEDs could be in volumetric illumination, such as 3D PTV or tomographic PIV. The design of the demonstrated LED line light is easily adaptable, for instance to manufacture a two-dimensional array of LEDs, which can illuminate volumes exceeding measurement regions illuminated by an expanded laser beam.

The development of more effective optical systems and LEDs with higher output will most certainly increase the applicability of these light sources as an alternative for laser-based illumination. The strong increase in light output will, on the other hand, induce the same restrictions as are present nowadays when using lasers to prevent skin- and eye damage. However, the radiation of an LED is always distributed throughout the width of the light sheet, whereas a laser contains all its radiation in a highly collimated, intense, small beam. Note that spreading of the laser beam into a light sheet may result in inhomogeneous illumination and shadowing of parts of the field-of-view, whereas an array of LEDs does not encounter these problems.

5. Conclusions

This work presents the development of a pulsed high power LED line light and its application as a light source to perform PIV measurements in a wave flume. A number of LEDs have been tested on their overdriving capabilities in pulsed operation, where the best performing type was able to withstand roughly 50 times its continuous load. An electrical circuit was developed to generate short, high intensity current pulses. And cylindrical lens setup was designed to collimate a bundle radiating from an array of LEDs, keeping the light sheet divergence limited ($\Delta z < 6$ mm for over 0.8 m) over a significant distance from the light source. Thereby providing constant homogeneous light conditions throughout a large area. These developments combined with an affordable CCD camera and open source PIV software, resulted in the successful application of an LED line light (of 0.6 m wide) to perform PIV measurements of the flow field of a wave impacting on an overhanging object.

From the analysis and results shown in this work it is concluded that a pulsed high-power LED line light can be applied as a light source for large-scale (0.7 $\times$ 0.7 m^2) planar PIV measurements to quantify the rapidly varying flow of a wave impacting on a blunt object with an overhang for velocities in the order of 1 m s^{-1}. The LED line light that is demonstrated is not necessarily eye-safe, but the emitted luminosity levels are significantly lower than in case conventional lasers are used for similar measurements. Furthermore its width is easily extendable (resulting in a larger light sheet) and it is less complex, vulnerable and expensive than a PIV laser. Moreover, due to the diverging and incoherent character of the LED light, the intensity levels drop rapidly with increasing distance from the LED source.

This work, gives a demonstration of a widely applicable, user-friendly, large-scale LED line light, with features (lens system, pulse width and LED line light length) that can be adapted to obtain the desired light sheet conditions.

Future developments in LEDs will result in an increase of luminous output, providing sufficient illumination for lower pulse widths and less diverging bundles.

Data availability statement

The data that support the findings of this study are available upon reasonable request from the authors.

Acknowledgment

This work was funded by the Netherlands Organisation for Scientific Research (NWO) under NWO Grant No.

ALWTW.2016.041. The authors kindly acknowledge the support that was provided. Furthermore the authors would like to thank Frank Kalkman for his assistance in designing and building the electrical circuit to generate high-current pulses.

ORCID iD

W Bakker https://orcid.org/0000-0002-5713-251X

References

[1] Adrian R J and Westerweel J 2011 *Particle Image Velocimetry* (Cambridge: Cambridge University Press)
[2] Adrian R J 2005 Twenty years of particle image velocimetry *Exp. Fluids* **39** 159–69
[3] Tropea C, Yarin A and Foss J F 2007 *Springer Handbook of Experimental Fluid Mechanics* (Berlin: Springer Science & Business Media)
[4] Bakker W, Verhaart F I H, de Fockert A and Oldenziel G 2019 Pulsed light emitting diodes for particle image velocimetry in a vertically submersible pump *38th Int. Association of Hydraulic Research World Congress (Panama City, Panama, 1–6 September)*
[5] Grayson K, de Silva C M, Hutchins N and Marusic I 2016 Laser light sheet profile and alignment effects on PIV performance *18th Int. Symp. on the Application of Laser and Imaging Techniques to Fluid Mechanics (Liston, Portugal, 4–7 July)*
[6] Ngoc-Hai V, Pham T T and Shin S 2017 LED Uniform Illumination using double linear Fresnel lenses for energy saving *Energies* **10** 1–15
[7] Wang G, Wang L, Li F and Zhang G 2012 Collimating lens for light-emitting-diode light source based on non-imaging optics *Appl. Opt.* **51** 1654–9
[8] Cornelius W 2000 ICNIRP Statement on light-emitting diodes (LEDS) and laser diodes: implications for hazard assessment *Health Phys.* **78** 744–52
[9] ICNIRP 2013 Guidelines on limits of exposure to incoherent visible and infrared radiation (0.38 to 3 μm) *Health Phys.* **105** 538–54
[10] Willert C, Stasicki B, Klinner J and Moessner S 2010 Pulsed operation of high-power light emitting diodes for imaging flow velocimetry *Meas. Sci. Technol.* **21** 075402
[11] Hagsäter S M, Westergaard C H, Bruus H and Kutter J P 2008 Investigations on LED illumination for micro-PIV including a novel front-lit configuration *Exp. Fluids* **44** 211–9
[12] Chételat O and Kim K C 2002 Miniature particle image velocimetry system with LED in-line illumination *Meas. Sci. Technol.* **13** 1006–13
[13] Lindken R, Rossi M, Grosse S and Westerweel J 2009 Micro-Particle Image Velocimetry (μPIV): recent developments, applications and guidelines *Lab Chip* **9** 2551–67
[14] Nasibov H, Balaban E, Kholmatov A and Nasibov A 2014 High-brightness, high-power LED-based strobe illumination for double-frame micro particle image velocimetry *Flow. Meas. Instrum.* **37** 12–28
[15] Aguirre-Pablo A A, Alarfaj M K, Qiang Li E, Hernandez-Sanchez J F and Thoroddsen S T 2017 Tomographic particle image velocimetry using smartphones and colored shadows *Sci. Rep.* **7** 3714
[16] Buchmann N A, Willert C and Soria J 2011 Tomographic particle image velocimetry using pulsed, high power LED volume illumination *9th Int. Symp. on Particle Image Velocimetry (Kobe, Japan, 21–23 July)*
[17] Harshani H M D, Galindo-Torres S A, Scheuermann A and Muhlhaus H B 2017 Experimental study of porous media flow using hydro-gel beads and LED based PIV *Meas. Sci. Technol.* **28** 015902
[18] Willert C E, Mitchell D M and Soria J 2012 An assessment of high-power light-emitting diodes for high frame rate schlieren imaging *Exp. Fluids* **53** 413–21
[19] Estevadeordal J and Goss L 2005 PIV with LED: particle shadow velocimetry (PSV) *43rd AIAA Aerospace Sciences Meeting and Exhibit (Reno, Nevada, 10–13 January)*
[20] Gross B, Brevis W and Jirka G H 2010 Development of a LED-based PIV/PTV system: characterization of the flow within a cylinder wall-array in a shallow flow *Int. Conf. of Fluival Hydraulics (Braunschweig, Germany, 8–10 September)*
[21] Pedrotti F L, Pedrotti L M and Pedrotti L S 2017 *Introduction to Optics* 3rd edn (Cambridge: Cambridge University Press)
[22] Atkinson A and Baldock T E 2016 A high-resolution sub-aerial and sub-aqueous laser based laboratory beach profile measurement system *Coast. Eng.* **107** 28–33
[23] Stanislas M, Westerweel J and Kompenhans J 2004 *Particle Image Velocimetry: Recent Improvements* (Berlin: Springer)
[24] de Almeida E and Hofland B 2020 Validation of pressure-impulse theory for standing wave impact loading on vertical hydraulic structures with short overhangs *Coast. Eng.* **159** 1–14
[25] Thielicke W and Stamhuis E J 2014 PIVlab—time-resolved digital particle image velocimetry tool for MATLAB (version: 2.31)
[26] Mathworks, Matlab R2020A 2020 Single camera calibration app (available at: www.mathworks.com/help/vision/ref/cameracalibrator-app.html (Accessed 20 March 2020)
[27] Westerweel J and Scarano F 2005 Universal outlier detection for PIV data *Exp. Fluids* **39** 1096–100
[28] Hochareon P, Manning K B, Fontaine A A, Tarbell J M and Deutsch S 2004 Wall shear-rate estimation within the 50cc Penn State artificial heart using particle image velocimetry *J. Biomech. Eng.* **126** 430–7
[29] Bastiaans R J M 1993 Cross-correlation PIV; theory, implementation and accuracy *EUT Reports* vol 99-W-001 (Eindhoven University of Technology)
[30] Stanislas M, Okamoto K and Kähler C 2003 Main results of the First Int. PIV Challenge *Meas. Sci. Technol.* **14** 63–89
[31] de Almeida E and Hofland B 2020 Experimental observations on impact velocity and entrapped air for standing wave impacts on vertical hydraulic structures with overhangs *J. Mar. Sci. Eng.* **8** 857–68
[32] Schuster R, Heitz D, Georgeault P and Mémin E 2020 On-site airflow measurement of a laboratory fume hood using customized large-scale image-based velocimetry *Indoor Built Environ.* **29** 810–9